PHILOSOPHICAL TRANSACTIONS A

rsta.royalsocietypublishing.org

Research

Article submitted to journal

Subject Areas:

Keywords:

Author for correspondence:
Dhrubaditya Mitra
email dhruba.mitra@gmail.com

Rate of formation of caustics in heavy particles advected by turbulence

Akshay Bhatnagar[1], Vikash Pandey[2], Prasad Perlekar[2], and Dhrubaditya Mitra[4]

[1] NORDITA, Royal Institute of Technology and Stockholm University, Stockholm.
[2] TIFR Centre for Interdisciplinary Sciences, Hyderabad.

The rate of collision and the relative velocities of the colliding particles in turbulent flows is a crucial part of several natural phenomena, e.g., rain formation in warm clouds and planetesimal formation in a protoplanetary disks. The particles are often modeled as passive, but heavy and inertial. Within this model, large relative velocities emerge due to formation of singularities (caustics) of in the gradient matrix of the velocities of the particles. Using extensive direct numerical simulations of heavy particles in both two (direct and inverse cascade) and three dimensional turbulent flows we calculate the rate of formation of caustics, J as a function of the Stokes number (St). The best approximation to our data is $J \sim \exp(-C/\mathrm{St})$, in the limit $\mathrm{St} \to 0$ where C is a non-universal constant.

1. Introduction

Turbulent flows in nature often have small particles embedded in them. Two canonical examples are gas flows in proto-planetary disks with small dust particles [1] and air flows in a cloud with small water droplets [2]. The first one is a useful model to understand the formation of planetesimals – small kilometer size objects that themselves collide and merge to form planets. The second one controls the physics of rain formation in warm clouds. In both of these cases a crucial problem is to understand the growth of few large objects from a lot of small ones. Let us consider the second case.

THE ROYAL SOCIETY PUBLISHING

Very small water droplets form by condensation in a super-saturated environment in the cloud. If only condensation and evaporation determines the evolution of the size of the droplets then, it can be estimated that, it would take unnaturally long for raindrops to form in a cloud [2]. Clearly, the droplets can also collide with each other and consequently merge or bounce off. The collision between droplets is determined by their relative velocities at small relative distances. If the velocity field of the droplets is smooth everywhere then the relative velocities between droplets go to zero as their relative distances go to zero. In this case, both the frequency of collisions and collision velocities remains small [3] and the estimated time to form raindrops is still unnaturally long. One way out of this conundrum is to consider the possibility that the velocity field of the droplets does not remain smooth but develop singularities – such that the relative velocity between two infinitesimally close droplets remains finite.

(a) Model

In the simplest case – the droplets are small and much heavier than the gas – the velocity of a single droplet in a flow satisfies the following equations:

$$\frac{d\boldsymbol{X}(t)}{dt} = \boldsymbol{V}(t), \tag{1.1a}$$

$$\frac{d\boldsymbol{V}(t)}{dt} = \frac{1}{\tau_{\rm p}}\left[\boldsymbol{u}(\boldsymbol{X},t) - \boldsymbol{V}\right], \tag{1.1b}$$

where $\boldsymbol{X}$ is the position, $\boldsymbol{V}$ is the velocity of the droplet, $\boldsymbol{u}$ is the velocity of the gas at a point $\boldsymbol{X}$, and $\tau_{\rm p} \equiv (2\rho_{\rm d}a^2)/(9\rho_{\rm g}\nu)$ is the relaxation time of the droplet. Here a is the radius of the droplet, ν is the kinematic viscosity of the gas, and $\rho_{\rm g}$ ($\rho_{\rm d}$) is the gas (droplet) density. We nondimensionalize $\tau_{\rm p}$ to introduce the Stokes number: ${\rm St} \equiv \tau_{\rm p}/\tau$, where τ is a characteristic time scale of turbulence. A small enough dust grain in a protoplanetary disk also obeys the same equations. To keep our discussions general, in the rest of this paper, we shall use the word "heavy inertial particle" to mean a water droplet or a dust grain small enough that their motion obeys (1.1).

In the Lagrangian frame of this heavy inertial particle the equation of evolution of the gradient of its velocity matrix, $\mathbb{Z}$, with components $Z_{\alpha\beta} \equiv \partial_\beta V_\alpha$ ($\alpha, \beta = 1, \ldots, d$ in d dimensions), is given by

$$\frac{dZ_{\alpha\beta}}{dt} + Z_{\alpha\gamma}Z_{\gamma\beta} + \frac{1}{\tau_{\rm p}}Z_{\alpha\beta} = \frac{1}{\tau_{\rm p}}A_{\alpha\beta}. \tag{1.2}$$

Where $A_{\alpha\beta} \equiv \partial_\beta u_\alpha$ are the components of the velocity-gradient matrix of the flow, $\mathbb{A}$, and repeated indices are summed. This equation contains the possibility that elements of $\mathbb{Z}$ can become infinitely large in finite time. To see this first consider the same equation in one dimension. Now both the particle velocity-gradient and the fluid velocity-gradients are scalars and (1.2) simplifies to

$$\frac{dZ}{dt} + Z^2 + \frac{1}{\tau_{\rm p}}Z = \frac{1}{\tau_{\rm p}}A, \tag{1.3}$$

where $Z \equiv \partial_x V$ and $A \equiv \partial_x u$. If we ignore the terms with coefficients equal to $1/\tau_p$ in (1.3), then for $Z(t=0) < 0$ the solution develops a finite-time singularity i.e. $Z \to -\infty$ in finite time $t = t_\star$. Such singularities have been named caustics [4]. We note that, in principle, (1.3) is an inappropriate model for flows in clouds because the incompressibility constraint ($\boldsymbol{\nabla}\cdot\boldsymbol{u} = 0$) dictates A to be identically zero. Let us, nevertheless, model the effects of turbulence in (1.3) by replacing A by a Gaussian, white-in-time noise. This turns (1.3) into a stochastic differential equation. From the corresponding Fokker-Planck equation Derevyanko et al. [5] evaluated the rate of formation of caustics

$$J \sim \exp\left(-\frac{C}{\tau_{\rm p}}\right), \tag{1.4}$$

where C is a constant. In two and three dimensions appearance of singularities implies that the trace of the matrix $\mathbb{Z}$ becomes infinitely large [6]. Blow-up of $\mathbb{Z}$ implies that two nearby particles

can have very high relative velocity [7,8]. In other words, inertial particles can detach from the flow. This effect is some times referred as sling effect [9].

2. Summary of earlier works

There is, by now, a significant volume of evidence from direct numerical simulations of turbulence that shows that a theory based on caustics correctly predicts the clustering and relative velocities of heavy particles [10–15]. Analytical calculations [5,8,9,16] of the rate of formation of caustics have been limited to one dimensional flows till very recently [17]. In such calculations the turbulence is approximated by a smooth random (Gaussian) flow with a length scale ℓ, correlation time T and velocity scale u. The gradient of flow velocity is assumed to be Gaussian. In addition to the Stokes number, this introduces another dimensionless number, the Kubo number: $\mathrm{Ku} \equiv uT/\ell$. In the limit $\mathrm{Ku} \to 0$ and $\mathrm{St} \to \infty$, such that the product $\mathrm{Ku}^2\mathrm{St}$ remains constant, the rate of formation of caustics is shown to be [16]: $J \sim \exp(-C/\mathrm{St})$. This limit also corresponds to solving (1.3) with a flow-gradient A that is random, Gaussian and white-in-time [5]. In the other limit – correlation time of A exceeds $1/A$ – $J \sim \exp(-C/\mathrm{St}^2)$ [9]. At finite Kubo numbers, Ref. [8] used a model where Z satisfies (1.3) and A satisfies an Ornstein–Uhlenbeck process. Numerical solution of this model and a WKB calculation showed that that the rate of formation of caustics depends on both St and Ku: (a) At small Kubo numbers $J \sim \exp(-C/\mathrm{St})$ for $St > 1$. (b) at larger Ku, e.g., at $\mathrm{Ku} = 1$, $J \sim \exp(-C/\mathrm{St}^2)$ in the limit $\mathrm{St} \to 0$.

Can we apply the results from these simple models to understand turbulent flows? Note that incompressible turbulent flows are either two or three dimensional. Numerical calculation for (1.2) in two and three dimensions [18] with a white-in-time $\mathbb{A}$ gives $J \sim \exp(-C/\mathrm{St})$. But turbulent flows are neither white-in-time nor do then remain correlated up to large times. Then, one possible way to relate these calculations to turbulent flows is to associate the characteristic length, velocity and the time scale of these synthetic flows with the length, velocity, and time scale at the Kolmogorov scale (also called the dissipative scale) respectively; hence $\mathrm{Ku} = 1$. But even at the dissipative scales a turbulent flows cannot be described by just one length scale [19], in other words there is not one unique Kolmogorov length scale. Furthermore, in turbulent flows the flow-gradient tensor, $\mathbb{A}$, obeys non-Gaussian statistics [20]. Hence, in summary, it is not obvious how to relate these analytical results to the turbulent flows. Cautiously, we expect the results in turbulent flows to be similar to those obtained for $\mathrm{Ku} = 1$, i.e., $J \sim \exp(-C/\mathrm{St}^2)$ as $\mathrm{St} \to 0$. As far as we are aware there has been so far no direct calculation of rate of formation of caustics in two-dimensional turbulence, although signatures of caustics has been observed in Eulerian simulations [21]. To the best of our knowledge, there is only one [22] calculation of the rate of formation of caustics in direct numerical simulations of three-dimensional turbulence. The calculation is for Taylor micro-scale Reynolds number of ranging from about 45 to 100. The authors claim $J \sim \exp(-C/\mathrm{St})$ but the conclusion is based on fitting a nonlinear function with four parameters to a data with seven points, see e.g. Ref. [23] for a criticism of a similar exercise. Here, we repeat their calculation for higher Reynolds numbers and improved statistics, in both two and three-dimension. In three dimension we use 10 million particles for each Stokes number.

3. Direct numerical simulations

We solve the Navier–Stokes equation in two and three dimensions with heavy inertial particles, (1.1) in the flow. In three dimensions we use the pencil-code [24,25]. The same code has been used in several earlier publications [12,13]. For the two-dimensional simulations we use a spectral code which has also been used in several earlier publications [26]. As the heavy inertial particles are much smaller than the energy containing scales of the flow, we use the Kolmogorov length scale ℓ_η and and time scale τ_η as our characteristic length and time scales respectively. We list the

relevant parameters of our simulations in table 1. In clouds the Stokes number [1] ranges from 0.01 to 2 for droplets of size 10 to 60 micrometer [27–29]. We use $\mathrm{St} = 0.1$ to 3.1 in three dimensions and $\mathrm{St} = 0.12$ to 1.1 in two-dimensions. In Table 2 we give a complete list of Stokes numbers used in each of our simulations. In two dimensions, depending on which length-scale is being forced, the turbulence may be dominated by either direct cascade of enstrophy (e.g., run $\mathtt{2d-R1}$) or inverse cascade of energy (e.g., run $\mathtt{2d-R8}$). In some two-dimensional simulations we have used a deterministic, Kolmogorov force in others we have used a stochastic, white-in-time, force. We have changed our Reynolds number over a large range, from approximately 150 to about 4000.

In addition to tracking the heavy inertial particles, we solve (1.2) on each of the particles. We choose $\mathbb{Z} = 0$, the zero matrix, on all the particles at $t = 0$. We count how many times the trace of $\mathbb{Z}$ ($\mathcal{T}r\,[\mathbb{Z}]$) crosses a large negative threshold, Z_{th} – we have used several values for this threshold. We define, the sum of all such crossing events over all the particles up to time t to be $N(t)$. The rate of formation of caustics

$$J(t) = \lim_{t\to\infty} \frac{N(t)}{t}. \tag{3.1}$$

4. Results

In Fig. 1(A) we plot $J(t)$ versus t for four different representative values of the Stokes number. At late times, $J(t)$ reaches a statistically stationary state. We consider the mean over this statistically stationary state as our measurement of the rate of formation of caustics and we use the maximum and minimum value of J over this statistically stationary state to set error limits. In Fig. 1(B) we plot the J as a function of St for both two and three dimensional simulations. In Fig. 1(C) we plot the logarithm of rate of formation of caustics $\log(J)$ as a function of $1/\mathrm{St}$ for all the runs. If (1.4) holds we expect to see a straight line as $1/\mathrm{St}$ becomes large. Clearly it is possible to fit such a line to the data for both two-dimensional and three-dimensional simulations. However, the fit is better for the three dimensional cases. For clarity we show two such fits to our data in Fig. 1(D). But we do not consider this a conclusive evidence in support of (1.4). In Fig. 1(C) we change the abscissa to $1/\mathrm{St}^2$. Here too it is possible to identify a region over which a straight line can be fit. This time the fit is marginally better for the two dimensional cases. To conclude, our data do not unequivocally support either $J \sim \exp(-C/\mathrm{St})$ or $J \sim \exp(-C/\mathrm{St}^2)$.

Equation 3.1 is not the only way to define the rate-of-formation of caustics. Let us define the time it takes for the trace of $\mathbb{Z}$ to exceed a threshold as the blow-up time tt_{b}. An alternative definition of rate-of-formation of caustics is $1/\langle t_{\mathrm{b}}\rangle$. Note that it is computationally more cumbersome to calculate the rate using this later definition. We have done it for only one of our runs, $\mathtt{2d-R2}$. In Fig. 2(A) we show the the cumulative probability distribution of the blow-up time $Q(t_{\mathrm{b}})$ calculated using the rank-order method [30], for several values of St. Clearly the distribution has exponential tail. In Fig. 2(B) we compare the two definitions of the rate-of-formation of caustics – they agree within error bars.

Singularities found in a numerical simulations are necessarily not true singularities – their detection depends on the threshold value we use. We have checked that by changing our threshold value $-Z_{\mathrm{th}}$ from 5 to 10^3 for the three-dimensional runs and from 10 to 10^{10} for the two-dimensional runs. The rate-of-formation of singularities itself changed, by small amounts, but its dependence on Stokes remains essentially unchanged. This is expected, because in (1.3) once $\mathcal{T}r\,[\mathbb{Z}] < -1/\tau_{\mathrm{p}}$ the dynamics is determined by Z^2. Hence any stochastic trajectories of $\mathbb{Z}$ where $\mathcal{T}r\,[\mathbb{Z}]$ becomes smaller than $-1/\tau_{\mathrm{p}}$ will reach blowup.

The numerical calculation of the rate of formation of caustics is a very difficult problem. We expect an asymptotic behaviour in the limit of small St but in this limit the rate of formation of caustics become exponentially small. This implies that to obtain reliable statistics at small St we either have to run our simulations for a very long time or for a very large number of particles. We have done the largest direct numerical simulations for calculation of caustics so far. We go

[1] The Kolmogorov time scale in clouds in estimated based on estimates of the energy-dissipation-rate, ε, which varies over a large range in different types of clouds. Consequently, the range of Stokes number for particles of the same size may be different in different clouds. The numbers we quote are typical of cumulus clouds.

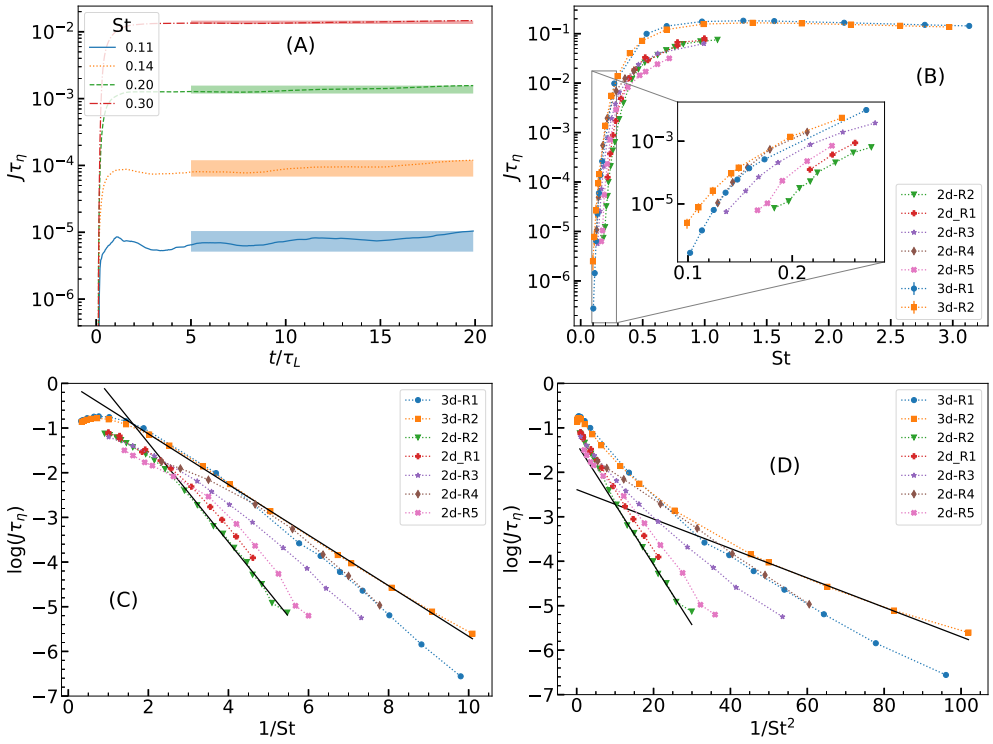

Figure 1. (A) The rate of formation of caustics $J(t)$ versus t for four different values of St. We calculate the mean value of J over the shaded region in each time series and set the maximum and minimum value of J as the error bars. (B) The rate of formation of caustics $J(t)$ as a function of St. The error bars are calculated according as shown in (A). They are smaller than the symbols. (C) The data in (B) plotted with $\log(\tau_\eta J)$ versus $1/\mathrm{St}$. (D) The data in (B) plotted with $\log(\tau_\eta J)$ versus $1/\mathrm{St}^2$. Notice that it is possible to find a range over which the plots show a linear trend in both (C) and (D). For clarity, we show such linear fits for two cases in each of (C) and (D).

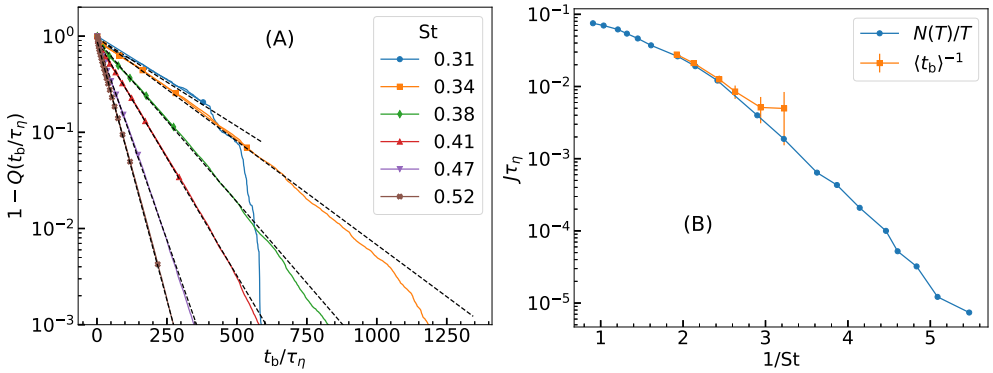

Figure 2. (A) The cumulative probability distribution function, $Q(t_\mathrm{b})$ (calculated using the rank-order method) of the blow-up time t_b for different values of the Stokes number (Run $\mathtt{2d-R2}$). The dashed lines are exponential fits to the tail of the data. The inverse of the mean of these data are plotted in (B) as a function of St and compared with the rate J calculated by counting the number of blow-ups, Eq. (3.1).

up to $\mathrm{Re}_\lambda = 180$ in three dimensions and $\mathrm{Re}_\lambda = 4100$ in two dimensions. In three-dimensional simulations we have used 10 million particles for each value of Stokes. In spite of such massive simulations we are unable to reach a definite conclusion on the asymptotic behaviour of the rate of formation of caustics. A recent paper [17], using analytical calculations in a two-dimensional model, where the gradient of flow-velocity is modeled by an Ornstein-Uhlenbeck process, shows that caustics tend to form for those particle trajectories that experience low values of vorticity of the flow and large values of rate-of-strain exceeding a threshold. Furthermore, two-dimensional direct numerical simulations agrees well with this result. In this paper, we have used the data from the same simulations but have not been able to reach a definite conclusion about the rate-of-formation of caustics.

Calculation of asymptotic behaviour from direct numerical simulations of turbulence is generally a quite challenging problem. For example, even in the case of stochastically forced Burgers equation in one dimension, where it is possible to run very high resolution simulations for a very long time, artifacts from sub-leading terms may make simple biscaling masquerade as multiscaling [31]. A scaling regime over a scaling range of at least a decade is considered necessary but not necessarily sufficient. An alternative is to use a seminumerical procedure called asymptotic extrapolation [32–34] that applies to the data a sequence of suitable chosen transformation that successively strip off dominant and subdominant terms. Following Ref. [32], we give a very short introduction to this procedure here.

Consider the general problem where we investigate whether a given numerical data can be fit with a function $G(r)$ with the leading order form

$$G(r) \sim C r^{-\alpha} e^{-\delta r}, \tag{4.1}$$

and thereby determine the parameters C, α and δ. One way is to ignore subleading corrections and try a least square fit. This is what we have done so far to the function $J(\mathrm{St})$. The parameters we obtain in this fashion sometime depends crucially on the fitting interval and determination of subleading corrections is almost impossible. The asymptotic extrapolation method allows, in principle, the determination of the asympotic expansion of the function $G(r)$, including the subleading terms, and an accurate determination of the parameters provided the numerical data is obtained with very high precision. A crucial feature of this procedure is that it uses the determination of subleading terms to improve the accuracy on leading-order terms

We describe below how we apply this procedure to our data. Let us assume that $J = \exp\left[-G(1/\mathrm{St})\right]$ with

$$G\left(n\right) \sim C n^{\alpha}(1 + \gamma_1 n + \gamma_2 n^2 \ldots) \tag{4.2}$$

We intend to extract the coefficients C, α, γ_1, etc systematically from the numerical data $G(n)$. We repeatedly iterate over G with a discrete operator $\boldsymbol{D}$ such that $G_{\mathrm{k}+1}(n) = \boldsymbol{D}G_{\mathrm{k}}(n) \equiv G_{\mathrm{k}}(n) - G_{\mathrm{k}}(n-1)$ and $G_0(n) = G(n)$. We show the results of repeated application of this operator on our data in Fig. 3. The left panel shows the results for our three dimensional simulations and the right panel shows the results for our two dimensional simulations. In both cases, we notice that G_2 is practically zero although in some cases with large noise. Inverting the operators imply that $G(n) \sim Cn$. Any coefficient of higher power of n is not discernible from the data. Consequently, our data, in both two and three dimensions, support $J \sim \exp(-C/\mathrm{St})$.

A word of caution is necessary here. The technique of asymptotic extrapolation is typically applied to data with high precision, otherwise repeated application of discrete operators, e.g., the difference operator we used, can get rid of the significant digits in the data and leave only noise. It has been used to study scaling of moments of gradients in direct numerical simulations of one dimensional Burgers equation [34] with both double and quadruple precision. For the case of double precision only three stages of iterations were possible. We have used double precision in all our calculations. We can iterate twice before the data became practically zero. This does not imply that there is no subdominant factor to $G(1/\mathrm{St})$. It rather means that the quality of our data does not allow us to extract any such contribution.

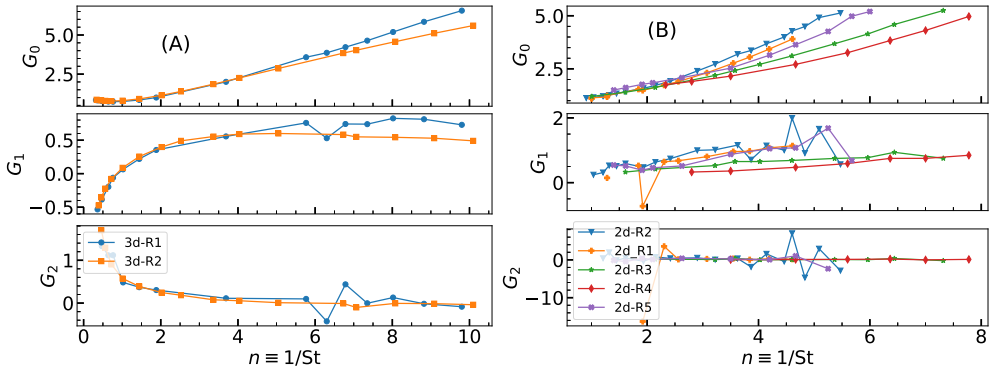

Figure 3. Results of successive application of the asymptotic extrapolation on three dimensional (left) and two dimensional (right) data. The zeroth function $G_0(n) \equiv -\log(\tau_\eta J)$ and $n = 1/\mathrm{St}$. In the next iteration $G_1(n) = D(G_0(n)) \equiv G_1(n) - G_1(n-1)$. In the next iteration $G_2(n) = D(G_1(n))$. In both cases, G_2 is asymptotically zero although there is a significant noise in some cases.

5. Conclusion

We have performed the highest resolution and most detailed study so far of the rate of formation of caustics in two and three-dimensional simulations of heavy inertial particles in turbulence. In spite of our diligence we have been unable to uncover how the rate of formation of caustics depends on the Stokes and Reynolds number. We find that a least-square fit to the data does not support unequivocally either of the two possibilities $J \sim \exp(-C/\mathrm{St})$ or $J \sim \exp(-C/\mathrm{St}^2)$. Next we applied the technique of asymptotic extrapolation to our data to find $J \sim \exp(-C/\mathrm{St})$. We do not consider this conclusive evidence. It is necessary to perform simulations at even smaller St with higher precision (at least quadruple precision). In the absence of definitive numerical evidence this remains an open problem.

Authors' Contributions. VP and AB have contributed equally to this work. DM and AB wrote the code for simulations in three dimensions. VP and PP wrote the code for simulations in two dimensions. All the four authors analyzed the data. DM drafted the manuscript with inputs from all the other authors. All authors read and approved the manuscript.

Competing Interests. The authors declare that they have no competing interests.

Funding. PP and VP acknowledge support from DST (India) Project Nos. ECR/2018/001135 and DST/NSM/R&D_HPC_Applications/2021/29. The computations were enabled by resources provided by the Swedish National Infrastructure for Computing (SNIC) at PDC partially funded by the Swedish Research Council through grant agreement no. 2018-05973. AB and DM acknowledges financial support from the grant Bottlenecks for particle growth in turbulent aerosols from the Knut and Alice Wallenberg Foundation (Dnr. KAW 2014.0048) and from Swedish Research Council Grant no. 638-2013-9243 as well as 2016-05225.

Acknowledgements. We have used matplotlib [35] to generate the figures in this paper. We thank Jan Meibohm and Bernhard Mehlig for discussions.

References

1. Armitage PJ. 2010 Astrophysics of Planet Formation. Cambridge, UK: Cambridge University Press.
2. Pruppacher H, Klett J. 2010 Microphysics of Clouds and Precipitation, volume 18. Springer Science & Business Media.
3. Saffman PG, Turner JS. 1956 On the collision of drops in turbulent clouds. Journal of Fluid Mechanics **1**, 16–30.
4. Wilkinson M, Mehlig B. 2003 Path coalescence transition and its applications. Physical Review E **68**, 040101.

Table 1. Parameters used in both our three dimensional simulations are listed here. The two-dimensional runs are marked with the prefix 2d and the three dimensional ones are marked with the prefix 3d. For the two dimensional runs we use a variety of different situations. Some of them are forced with a deterministic Kolmogorov force, some are forced with a stochastic force. The force is always limited to a a single wave-number $k_{\rm f}$. For a small $k_{\rm f}$ we develop a direct cascade, whereas for a large $k_{\rm f}$ we develop a large range of inverse cascade. We also change the threshold of detection of singularities, $Z_{\rm th}$, which has no appreciable effect on the dependence of J (rate of formation of singularities) on the Stokes number. The rate of formation of caustics from these runs are plotted in Fig. 1. Definition of symbols: $\mathtt{N}$, number of grid points in one direction, 2-d runs have $\mathtt{N}^2$ number of grid points and 3-d runs have $\mathtt{N}^3$ grid points; dt, time-step used in the 2-d solver. ν, viscosity; μ, Ekman friction; f_0, amplitude of the force; $\langle\cdot\rangle$, spatial average over the computational box and temporal average over the statistically-stationary, non-equilibrium, state of turbulence; $u_{\rm rms}=\sqrt{\langle \boldsymbol{u}^2\rangle/d}$ ($d=2,3$ is the dimension), the root-mean-square velocity of the flow; $k_{\rm f}$, the forcing wavenumber; $\mathcal{L}_{\rm I}\equiv 2\pi/k_{\rm f}$, the integral scale; $T_{\mathcal{L}}=\mathcal{L}_{\rm I}/u_{\rm rms}$, the large-eddy-turnover-time; $\boldsymbol{\omega}=\boldsymbol{\nabla}\times\boldsymbol{u}$, the vorticity; $\Omega=\langle\boldsymbol{\omega}^2\rangle/2$, the enstrophy; $\omega_{\rm rms}=\sqrt{(2/3)\Omega}$ in 3-d and $\omega_{\rm rms}=\sqrt{2\Omega}$ in 2-d is the root-mean-square vorticity; $\varepsilon=2\nu\Omega$, the rate of energy dissipation; $\eta\equiv(\nu^3/\varepsilon)^{1/4}$, Kolmogorov (dissipation) length scale, $\lambda=u_{\rm rms}/\omega_{\rm rms}$, the Taylor microscale; ${\rm Re}_\lambda=u_{\rm rms}\lambda/\nu$, the Taylor microscale Reynolds number; ${\rm St}=\tau_{\rm p}/\tau_\eta$, the Stokes number. We use ${\rm St}=0.1$ to 3.1 in three-dimensions and ${\rm St}=0.12$ to 1.1 in two dimensions. All the values of St used in different runs are given in table 2.

$runs$	$\mathtt{N}$	${\rm Re}_\lambda$	τ_η	η	$k_{\rm f}$	$T_{\mathcal{L}}$	μ	dt
$\mathtt{2d-R1}$	512	395	4.6	0.007	4	36.8	0.01	5×10^{-3}
$\mathtt{2d-R2}$	1024	1311	2.9	0.005	4	21.0	0.01	5×10^{-3}
$\mathtt{2d-R3}$	1024	360	1.6	0.004	35	3.7	0.001	5×10^{-3}
$\mathtt{2d-R4}$	1024	73	1.4	0.0037	100	1.0	0.0002	5×10^{-3}
$\mathtt{2d-R5}$	1024	4100	2.1	0.005	2 - 3	17.7	0.01	1×10^{-3}
$\mathtt{3d-R1}$	512	90	0.39	0.014	5	5.46	—	—
$\mathtt{3d-R2}$	512	170	1.56	0.014	2	36.98	—	—

Table 2. Values of St used in different simulations

$runs$	St
$\mathtt{2d-R1}$	0.22, 0.24, 0.26, 0.28, 0.32, 0.39, 0.43, 0.52, 0.54, 0.78
$\mathtt{2d-R2}$	0.18, 0.20, 0.21, 0.22, 0.24, 0.26, 0.28, 0.31, 0.34, 0.41, 0.46, 0.52, 0.62, 0.69, 0.76, 0.83, 0.97, 1.10
$\mathtt{2d-R3}$	0.14 0.15, 0.17, 0.19, 0.22, 0.25, 0.28, 0.31, 0.47, 0.62, 1.00
$\mathtt{2d-R4}$	0.13, 0.14, 0.16, 0.18, 0.21, 0.29, 0.36, 0.43
$\mathtt{2d-R5}$	0.17, 0.18, 0.19, 0.21, 0.24, 0.29, 0.38, 0.48, 0.52, 0.62, 0.71
$\mathtt{3d-R1}$	0.10, 0.11, 0.12, 0.14, 0.15, 0.16, 0.17, 0.27, 0.53, 0.69, 0.98, 1.31, 1.56,2.12, 2.77, 3.13
$\mathtt{3d-R2}$	0.10, 0.11, 0.12, 0.14, 0.15, 0.20, 0.25, 0.30, 0.40, 0.50, 0.70, 0.90, 1.40, 1.79, 2.19, 2.59

5. Derevyanko S, Falkovich G, Turitsyn K, Turitsyn S. 2007 Lagrangian and eulerian descriptions of inertial particles in random flows.
Journal of Turbulence p. N16.
6. Gustavsson K, Mehlig B. 2016 Statistical models for spatial patterns of heavy particles in turbulence.
Advances in Physics **65**, 1–57.
7. Gustavsson K, Mehlig B. 2011 Distribution of relative velocities in turbulent aerosols.
Physical Review E **84**, 045304.
8. Gustavsson K, Mehlig B. 2013 Distribution of velocity gradients and rate of caustic formation in turbulent aerosols at finite kubo numbers.
Physical Review E **87**, 023016.
9. Falkovich G, Fouxon A, Stepanov M. 2002 Acceleration of rain initiation by cloud turbulence.
Nature **419**, 151–154.
10. Voßkuhle M, Pumir A, Lévêque E, Wilkinson M. 2014 Prevalence of the sling effect for enhancing collision rates in turbulent suspensions.

Journal of fluid mechanics **749**, 841–852.
11. Perrin VE, Jonker HJ. 2015 Relative velocity distribution of inertial particles in turbulence: A numerical study.
Physical Review E **92**, 043022.
12. Bhatnagar A, Gustavsson K, Mitra D. 2018 Statistics of the relative velocity of particles in turbulent flows: Monodisperse particles.
Physical Review E **97**, 023105.
13. Bhatnagar A, Gustavsson K, Mehlig B, Mitra D. 2018 Relative velocities in bidisperse turbulent aerosols: Simulations and theory.
Physical Review E **98**, 063107.
14. Rani SL, Dhariwal R, Koch DL. 2019 Clustering of rapidly settling, low-inertia particle pairs in isotropic turbulence. part 2. comparison of theory and dns.
Journal of Fluid Mechanics **871**, 477–488.
15. Dhariwal R, Bragg AD. 2018 Small-scale dynamics of settling, bidisperse particles in turbulence.
Journal of Fluid Mechanics **839**, 594–620.
16. Wilkinson M, Mehlig B, Bezuglyy V. 2006 Caustic activation of rain showers.
Physical review letters **97**, 048501.
17. Meibohm J, Pandey V, Bhatnagar A, Gustavsson K, Mitra D, Perlekar P, Mehlig B. 2020 Paths to caustic formation in turbulent aerosols.
arXiv preprint arXiv:2012.08424 .
18. Wilkinson M, Mehlig B, Östlund S, Duncan K. 2007 Unmixing in random flows.
Physics of Fluids **19**, 113303.
19. Schumacher J, Sreenivasan KR, Yakhot V. 2007 Asymptotic exponents from low-reynolds-number flows.
New Journal of Physics **9**, 89.
20. Chevillard L, Meneveau C. 2006 Lagrangian dynamics and statistical geometric structure of turbulence.
Physical review letters **97**, 174501.
21. Mitra D, Perlekar P. 2018 Topology of two-dimensional turbulent flows of dust and gas.
Physical Review Fluids **3**, 044303.
22. Falkovich G, Pumir A. 2007 Sling effect in collisions of water droplets in turbulent clouds.
Journal of the Atmospheric Sciences **64**, 4497–4505.
23. Dyson F. 2004 A meeting with enrico fermi.
Nature **427**, 297–297.
24. Brandenburg A, Dobler W. 2002 Hydromagnetic turbulence in computer simulations.
Computer Physics Communications **147**, 471–475.
25. Pencil Code Collaboration, Brandenburg A, Johansen A, Bourdin P, Dobler W, Lyra W, Rheinhardt M, Bingert S, Haugen N, Mee A, Gent F, Babkovskaia N, Yang CC, Heinemann T, Dintrans B, Mitra D, Candelaresi S, Warnecke J, Käpylä P, Schreiber A, Chatterjee P, Käpylä M, Li XY, Krüger J, Aarnes J, Sarson G, Oishi J, Schober J, Plasson R, Sandin C, Karchniwy E, Rodrigues L, Hubbard A, Guerrero G, Snodin A, Losada I, Pekkilä J, Qian C. 2021 The pencil code, a modular mpi code for partial differential equations and particles: multipurpose and multiuser-maintained.
Journal of Open Source Software **6**, 2807.
26. Pandey V, Perlekar P, Mitra D. 2019 Clustering and energy spectra in two-dimensional dusty gas turbulence.
Physical Review E **100**, 013114.
27. Shaw RA. 2003 Particle-turbulence interactions in atmospheric clouds.
Annual Review of Fluid Mechanics **35**, 183–227.
28. Ayala O, Rosa B, Wang LP, Grabowski WW. 2008 Effects of turbulence on the geometric collision rate of sedimenting droplets. part 1. results from direct numerical simulation.
New Journal of Physics **10**, 075015.
29. Grabowski WW, Wang LP. 2013 Growth of cloud droplets in a turbulent environment.
Annual Review of Fluid Mechanics **45**, 293–324.
30. Sharma R, Mitra D, Oberoi D. 2017 On the energization of charged particles by fast magnetic reconnection.
Monthly Notices of the Royal Astronomical Society **470**, 723–731.

31. Mitra D, Bec J, Pandit R, Frisch U. 2005 Is multiscaling an artifact in stochastically forced burgers equation ?
Phys. Rev. Lett **94**, 194501.
32. Pauls W, Frisch U. 2007 A borel transform method for locating singularities of taylor and fourier series.
Journal of Statistical Physics **127**, 1095–1119.
33. van der Hoeven J. 2009 On asymptotic extrapolation.
Journal of Symbolic Computation **44**, 1000–1016.
34. Chakraborty S, Frisch U, Pauls W, Ray SS. 2012 Nelkin scaling for the burgers equation and the role of high-precision calculations.
Physical Review E **85**, 015301.
35. Hunter JD. 2007 Matplotlib: A 2d graphics environment.
Computing in Science & Engineering **9**, 90–95.